JCTC Journal of Chemical Theory and Computation

Article

pubs.acs.org/JCTC

Representability and Transferability of Kirkwood−Buff Iterative Boltzmann Inversion Models for Multicomponent Aqueous Systems

Pritam Ganguly and Nico F. A. van der Vegt*

Center of Smart Interfaces, Technische Universität Darmstadt, Alarich-Weiss-Strasse 10, 64287 Darmstadt, Germany

Supporting Information

ABSTRACT: We discuss the application of the Kirkwood−Buff iterative Boltzmann inversion (KB-IBI) method for molecular coarse-graining (Ganguly et al. *J. Chem. Theory Comput.* **2012**, *8*, 1802) to multicomponent aqueous mixtures. Using a fixed set of effective single-site solvent−solvent potentials previously derived for binary urea−water systems, solute−solvent and solute−solute KB-IBI coarse-grained (CG) potentials have been derived for benzene in urea−water mixtures. Preferential solvation and salting-in coefficients of benzene are reproduced in quantitative agreement with the atomistic force field model. The transferability of the CG models is discussed, and it is shown that free energies of formation of hydrophobic benzene clusters obtained from simulations with the CG model are in good agreement with results obtained from all-atom simulations. The state-point representability of the CG models is discussed with respect to reproducing thermodynamic quantities such as pressure, isothermal compressibility, and preferential solvation. Combined use of KB-IBI and pressure corrections in deriving single-site CG models for pure-water, binary mixtures of urea and water, and ternary mixtures of benzene in urea−water at infinite benzene dilution provides an improved scheme to representing the atomistic pressure and the preferential solvation between the solution components. It is also found that the application of KB-IBI leads to a faster and improved convergence of the pressure and potential energy compared to the IBI method.

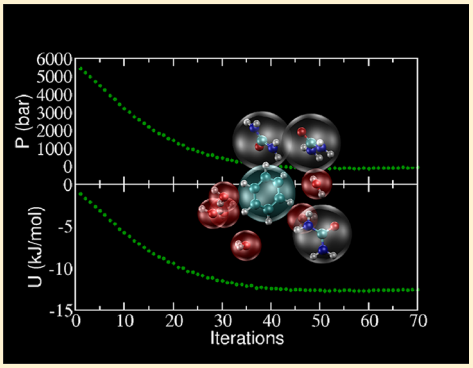

1. INTRODUCTION

Molecular simulations with detailed atomistic models frequently face limitations in sampling condensed phase systems on sufficiently long time and length scales. While on the one hand chemical specificity is often required, computational efficiency and speed are required on the other hand. Among many other examples, a process such as a conformational transition of a solvated macromolecule or protein driven by variations in the thermodynamic activity of (co)solvent components clearly calls for models that are simple yet specific. While coarse-grained (CG) models may potentially bridge several orders in time and length scales, it remains a significant challenge to develop representative CG models for complex molecular systems that are sufficiently transferable such that they can be used in multiscale simulations of soft matter systems under equilibrium and nonequilibrium conditions. Clearly, these types of questions require CG models that reproduce some of the structural and thermodynamic properties of the atomistic system, a requirement which is not straightforwardly met in general.[1−4] While systematic (bottom up) coarse-graining approaches to develop structurally consistent and transferable CG models for molecular liquids and macromolecules exist in the literature,[5−13] significantly less attention has been devoted to deriving CG potentials for molecular mixtures, in particular for aqueous solution systems that contain cosolvent components. Systematic coarse-graining approaches that include preferential solvation in the parametrization procedure, in addition to other structural and thermodynamic properties, may provide new routes to modeling these complex systems at a CG level.

In recent years, the iterative Boltzmann inversion (IBI) method[14,15] has gained significant popularity as it provides a robust tool to derive structure-based CG models for condensed phase systems. The method iteratively improves an effective pair potential until agreement is found between the pair correlation functions at the atomistic and CG level of modeling. The derived potential is in principle unique, as stated by the Henderson theorem,[16] which shows that two different pair potentials that generate the same radial distribution function (RDF) can differ by a constant only. In practical applications of IBI it has however been shown that two very different pair potential functions can produce two very similar RDFs which are indistinguishable within very small error margins.[17] Although this suggests that the IBI method is an ill-posed inverse mathematical problem, it provides some additional flexibility to optimize the effective pair potentials in such a way that not only target RDFs are reproduced but also other thermodynamic "target quantities" such as the energy or pressure, which are both sensitive to variations in the tails of the effective pair potentials.[15] It should be noted though that different thermodynamic targets cannot always be satisfied

Received: March 26, 2013
Published: November 5, 2013

   dx.doi.org/10.1021/ct400242r | *J. Chem. Theory Comput.* 2013, 9, 5247−5256

independently, thus requiring a "best compromise" to be found. For example, it is difficult (if not impossible) to match, both, the pressure and the isothermal compressibility of liquid water with single-site IBI models.[18] For more simple systems with Lennard-Jones interactions only, it has been found that by using a minimization procedure that matches the RDF and the pressure, an improvement is achieved in reproducing the isothermal compressibility.[19] For solution mixtures, these aspects have so far not been addressed in the literature.

In this paper, we discuss some aspects of the representability and transferability of IBI-based CG models for molecular mixtures with emphasis on aspects of preferential solvation and corresponding thermodynamic changes that lead to salting-in of a model hydrophobic solute. We study the solvation and salting-in of benzene in urea−water mixtures where the interactions will be described by means of single-site CG models. Studies of solutes in the mixtures of urea and water are chosen in this work because urea is a well-known chemical denaturant for proteins[20−23] and preferentially interacts with hydrophobic groups[24,25] and peptide backbones.[23,26,27] Biomacromolecules in water can be unfolded upon addition of urea because of the preferential binding of urea to the polar and the nonpolar groups which favors solvent exposure of these groups and decreases the solvation free-energy of the macromolecules in water. In this paper the salting-in of benzene in urea−water solutions will be studied at different urea concentrations (from 6 to 12 m) at infinite solute dilution and at two finite solute concentrations for benzene in 4−8 *m* urea−water solution. We use the binary urea/water CG solvent model derived previously[28] and newly parametrize solute−solvent, solute−cosolvent, and solute−solute interactions. We also report the free-energy associated with the growth of the benzene clusters in urea−water mixtures with all-atom (AA) and CG models. In addition to that we also study the representability of the structure-based CG models in terms of pressure and isothermal compressibility and the respective convergence of the thermodynamic quantities such as average potential energy per molecule for the systems of pure water, binary mixtures of urea and water, and ternary mixtures of benzene in urea−water at infinite benzene dilution.

2. KIRKWOOD−BUFF ITERATIVE BOLTZMANN INVERSION

In a previous study,[28] single-site models of urea in water have been developed where the CG models were able to reproduce (with respect to the atomistic simulations) the pair correlations between solution components as well as the derivatives of the solvation free energies of urea in water with varying urea concentration. In that paper, the authors proposed a new method for coarse-graining, called Kirkwood−Buff iterative Boltzmann inversion (KB-IBI), which uses the reference (atomistic) RDFs and the integrals of the RDFs over volume, called Kirkwood−Buff integrals (KBIs), as target properties to develop CG potentials iteratively. The method can be understood as an extension of IBI and uses KBIs as additional target quantities in the derivation of the CG models. The rationale behind this method lies in the Kirkwood−Buff theory,[29] which relates KBIs to the macroscopic thermodynamic quantities like isothermal compressibility, partial molar volumes, and derivatives of chemical potentials or activity coefficients with composition through KBIs (G_{ij}) defined as

$$G_{ij} = 4\pi \int_0^\infty [g_{ij}(r) - 1] r^2 \mathrm{d}r \tag{1}$$

where $g_{ij}(r)$ is the RDF and G_{ij} the KBI between the particle types i and j present in the system. The KBI can physically be interpreted as the affinity between the particle types *i* and *j* and $\rho_j G_{ij}$ gives the excess coordination number of particle type *j* around particle type *i*, where ρ_j is the particle number density of particle type *j*. In a binary system of solvent (water(w)) and cosolvent (urea(u)) the variation in the molar activity coefficient (γ_u) of the cosolvent at constant pressure *p* and temperature *T* is given by[30]

$$\left(\frac{\partial \ln \gamma_u}{\partial \ln \rho_u}\right)_{p,T} = -\frac{\rho_u(G_{uu} - G_{uw})}{1 + \rho_u(G_{uu} - G_{uw})} \tag{2}$$

where ρ_u is the cosolvent number density. Similarly, in a ternary system with solute (b), solvent (w), and cosolvent (u), the KBIs can be related to the derivative of the solvation free-energy (ΔG_b) of the solute with respect to the change in the mole fraction of the cosolvent (x_u) at infinite solute dilution:

$$\lim_{\rho_b \to 0}\left(\frac{\partial \Delta G_b}{\partial x_u}\right)_{p,T} = \frac{RT(\rho_w + \rho_u)^2}{\eta}(G_{bw} - G_{bu}) \tag{3}$$

where *R* is the gas constant, $\eta = \rho_w + \rho_u + \rho_w\rho_u(G_{ww} + G_{uu} - 2G_{uw}) > 0$ for stable solutions, and "ρ"s are the number densities of the components present in the system. If the cosolvent affinity of the solute (G_{bu}) exceeds its water affinity (G_{bw}), in other words, if $G_{bu} > G_{bw}$, then $(\partial \Delta G_b/\partial x_u)_{p,T} < 0$, i.e., the solvation free-energy of the solute decreases with increasing cosolvent concentration. This phenomenon is called "salting-in". The opposite phenomenon where $G_{bu} < G_{bw}$, is referred to as "salting-out" and corresponds to preferential hydration of the solute. Benzene is salted-in by urea in water.[31] From eqs 2 and 3 it is clear that to study the salting-in processes of the solute with CG descriptions we need to have CG models which reproduce the respective KBIs. The KB-IBI method has been introduced to provide CG potentials that reproduce RDFs and KBIs in mixtures and is therefore particularly useful in this context.

3. SIMULATION DETAILS

All-atom systems were simulated using GROMACS molecular dynamics (MD) package.[32] For urea a Kirkwood−Buff derived force-field was used.[33] Gromos43a1 parameters[34] for benzene were used. Water was simulated with the SPC/E potential.[36] NpT simulations were performed at a temperature of 300 K and a pressure of 1 bar. The temperature was controlled using a Nose−Hoover thermostat[37,38] with a relaxation time of 0.5 ps. The pressure was kept constant using the Parrinello−Rahman barostat[39] with a coupling time of 3 ps. The particle mesh Ewald (PME)[40] method was used for calculating the electrostatic interactions. The cutoff radius for all nonbonded interactions was set at 1 nm. The equations of motion were integrated using a leapfrog integrator with a 2 fs time-step, and 100 ns long trajectories were obtained for all the binary and ternary mixtures, and the last 90 ns were used for analysis. A 5 ns long trajectory was used for pure water. For all the simulations of the binary and ternary mixtures cubic boxes with periodic boundary conditions containing 11111 water molecules were studied, the number of the benzene and urea

Table 1. Comparison between the Atomistic and Coarse-Grained (KB-IBI) Force Fields in Terms of the KBIs and the Derivatives of the Solvation Free-Energy or Chemical Potential of Benzene with Varying Urea Concentrations[a]

system	N_u	N_b	N_w	G_{bw} (nm^3)	G_{bu} (nm^3)	G_{bb} (nm^3)	G_{uu} (nm^3)	G_{uw} (nm^3)	G_{ww} (nm^3)	$(\partial\Delta G_b/\partial x_u)_{p,T,\rho_b\to 0}$ (kJ/mol)	$(\partial\mu_b/\partial N_u)_{p,T}$ (kJ/mol)
6, dil (AA)	1200	1	11111	−0.221	0.168	–	−0.064	−0.079	−0.015	−23.4	–
6, dil (CG)[b]	1200	1	11111	−0.221	0.151	–	−0.069	−0.076	−0.014	−22.1	–
6, dil(cG)[g]	1200	1	11111	−0.208	0.130	–	−0.073	−0.075	−0.015	−21.1	–
6, dil (CG)[h]	1200	1	11111	−0.220	0.182	–	−0.056	−0.084	−0.005	−22.8	–
8, dil (AA)	1600	1	11111	−0.180	−0.021	–	−0.077	−0.074	−0.012	−9.3	–
8, dil(CG)[c]	1600	1	11111	−0.178	−0.003	–	−0.070	−0.077	−0.011	−9.9	–
10, dil (AA)	2000	1	11111	−0.190	−0.026	–	−0.090	−0.069	−0.011	−9.8	–
10, dil(CG)[d]	2000	1	11111	−0.186	−0.018	–	−0.086	−0.070	−0.010	−9.8	–
12, dil (AA)	2400	1	11111	−0.214	−0.002	–	−0.099	−0.066	−0.010	−12.7	–
12, dil(CG)[e]	2400	1	11111	−0.210	−0.008	–	−0.084	−0.070	−0.006	−10.7	–
4, 0.25 (AA)	800	50	11111	−0.199	0.137	0.407	−0.027	−0.088	−0.015	–	−0.00193
4, 0.25 (CG)[f]	800	50	11111	−0.221	0.275	0.668	−0.067	−0.084	−0.014	–	−0.00280
4, 0.25 (CG)[g]	800	50	11111	−0.205	0.150	0.880	−0.066	−0.070	−0.015	–	−0.00207
6, 0.25 (AA)	1200	50	11111	−0.232	0.139	0.759	−0.062	−0.082	−0.010	–	−0.00187
6, 0.25 (CG)[f]	1200	50	11111	−0.253	0.234	0.751	−0.066	−0.083	−0.009	–	−0.00239
6, 0.25 (CG)[g]	1200	50	11111	−0.223	0.137	0.738	−0.065	−0.082	−0.010	–	−0.00184
8, 0.25 (AA)	1600	50	11111	−0.228	0.076	0.460	−0.081	−0.075	−0.008	–	−0.00155
8, 0.25 (CG)[f]	1600	50	11111	−0.280	0.236	0.282	−0.062	−0.084	−0.003	–	−0.00230
8, 0.25 (CG)[g]	1600	50	11111	−0.270	0.194	0.793	−0.063	−0.084	−0.004	–	−0.00199
4, 0.50 (AA)	800	100	11111	−0.237	0.187	0.793	−0.040	−0.092	−0.009	–	−0.00205
4, 0.50 (CG)[g]	800	100	11111	−0.243	0.154	1.074	−0.076	−0.084	−0.009	–	−0.00195
6, 0.50 (AA)	1200	100	11111	−0.247	0.116	0.775	−0.064	−0.087	−0.004	–	−0.00165
6, 0.50 (CG)[f]	1200	100	11111	−0.286	0.275	0.875	−0.061	−0.092	−0.001	–	−0.00240
6, 0.50 (CG)[g]	1200	100	11111	−0.243	0.174	0.601	−0.066	−0.086	−0.004	–	−0.00196
8, 0.50 (AA)	1600	100	11111	−0.254	0.069	0.857	−0.085	−0.076	−0.002	–	−0.00142
8, 0.50 (CG)[g]	1600	100	11111	−0.263	0.131	0.749	−0.065	−0.085	0.001	–	−0.00160

[a]Subscripts b, u, and w stand for benzene, urea, and water, respectively. G_{ij}'s are the KBIs, and N_i's are the numbers of the molecules of different species. $(\partial\Delta G_b/\partial x_u)_{p,T,\rho_b\to 0}$ is the derivative of the solvation free-energy of benzene with varying urea mole fraction at infinite dilution of benzene, and $(\partial\mu_b/\partial N_u)_{p,T}$ is the derivative of the chemical potential of benzene with number of urea molecules at finite concentrations of benzene. The labels for the systems denote the molal concentrations of urea and benzene respectively (6, 0.25 being 0.25 *m* benzene in 6 *m* urea−water solution; dil: infinite dilution of benzene). AA: all-atom; CG: coarse-grained. Footnotes *b*−*h* refer to the different KB-IBI coarse-graining schemes. [b]Urea−urea, urea−water, and water−water potentials are obtained by KB-IBI method from binary mixture of 6 *m* urea in water; benzene−urea and benzene−water potentials are parametrized from single benzene molecule in 6 *m* urea−water using KB-IBI. [c]Urea−urea, urea−water, and water−water potentials are obtained by KB-IBI method from binary mixture of 6 *m* urea in water; benzene−urea and benzene−water potentials are parametrized from single benzene molecule in 8 *m* urea−water using KB-IBI. [d]Urea−urea, urea−water, and water−water potentials are obtained by KB-IBI method from binary mixture of 10 *m* urea in water; benzene−urea and benzene−water potentials are parametrized from single benzene molecule in 10 *m* urea−water using KB-IBI. [e]Urea−urea, urea−water, and water−water potentials are obtained by KB-IBI method from binary mixture of 10 *m* urea in water; benzene−urea and benzene−water potentials are parametrized from single benzene molecule in 12 *m* urea−water using KB-IBI. [f]Urea−urea, urea−water, and water−water potentials are obtained by KB-IBI method from binary mixture of 6 *m* urea in water; benzene−urea and benzene−water potentials are parametrized from single benzene molecule in 6 *m* urea−water using KB-IBI; benzene−benzene potential is obtained from 0.25 *m* benzene in 6 *m* urea−water solution. [g]Urea−urea, urea−water, and water−water potentials are obtained by KB-IBI method from binary mixture of 6 *m* urea in water; benzene−urea, benzene−water, and benzene−benzene potentials are obtained from 0.25 *m* benzene in 6 *m* urea−water solution. [h]Urea−urea, urea−water, and water−water potentials are obtained by KB-IBI method from binary mixture of 6 *m* urea in water with pressure corrections applied to water−water potential; benzene−urea and benzene−water potentials are parametrized from single benzene molecule in 6 *m* urea−water using KB-IBI.

molecules was varied accordingly (details of the numbers of the molecules are listed in Table 1). The linear dimension of the cubic simulation boxes varied between 7.5 and 8.0 nm. Simulation of pure water was performed using 2180 water molecules, corresponding to a box size of 4.0 nm.

All CG MD simulations were performed with the GROMACS package. A leapfrog stochastic algorithm was used with an inverse friction constant of 0.2 ps. Coarse-grained systems were simulated under constant NVT conditions (300 K) where the average volumes of the corresponding atomistic simulations were used. The time step for integration was 4 fs, and 20 ns long trajectories were accumulated. The cutoff for nonbonded interactions was set to 1.4 nm. Parametrization of the CG force-fields, both for IBI and KB-IBI, was done using VOTCA 1.2 package.[41] For the ternary mixtures of benzene, urea, and water 40−60 KB-IBI iterations were preceded by 30 iterations of IBI (with 10 ns long simulations per iteration for IBI and KB-IBI). Pressure and KB-IBI ramp corrections for the binary urea−water mixture were performed with 2 ns long trajectories per iteration, while for pure water all the parametrizations were done with 0.5 ns trajectories per iteration. The prefactors of the KB-IBI ramp-potentials[28] were chosen to be ≈0.5 kJ nm^{-3} mol^{-1} for the potentials involving benzene, ≈0.4 kJ nm^{-3} mol^{-1} for the potentials involving urea in the binary urea−water systems, and ≈10.0 kJ nm^{-3} mol^{-1} for the systems with pure water.

Atomistic and CG KBIs were calculated by taking the average of the running KBIs ($G_{ij}(r) = 4\pi\int_0^r[g_{ij}(s) - 1]s^2ds$, r being the radial distance) between r = 1.0 and 1.4 nm.

4. RESULTS AND DISCUSSION

4.1. Salting-in at Infinite Solute Dilution. To study salting-in of the solute at infinite dilution in urea−water solutions with CG single-site models, we have run both atomistic and CG simulations of urea−water using simulation boxes with varying urea concentrations containing just one solute (benzene) molecule. For all the CG systems, the solvent models (effective pair potentials for urea−urea, urea−water, and water−water interactions at different urea concentrations) were taken from the simulations of binary urea−water solutions,[28] while the solute−solvent and solute−cosolvent potentials (solute−urea and solute−water) were newly obtained. Systems with a single benzene molecule in urea−water solution were studied with four different urea concentrations, namely 6, 8, 10, and 12 m (molality). For the simulations of 6 and 8 m urea we used the CG solvent model previously derived for pure urea−water solutions at 6 m urea concentration.[28] For the systems with 10 and 12 m urea, the CG solvent model[28] derived at 10 m urea concentration was used. This choice reflects the concentration transferability of the CG urea/water model which is limited to ∼2 m concentration windows. For all concentrations of urea, the solute−solvent interactions (benzene−urea and benzene−water) were parametrized using KB-IBI. The solute−solvent KB-IBI potentials obtained at 6 and 10 m urea are shown in Figure 1.

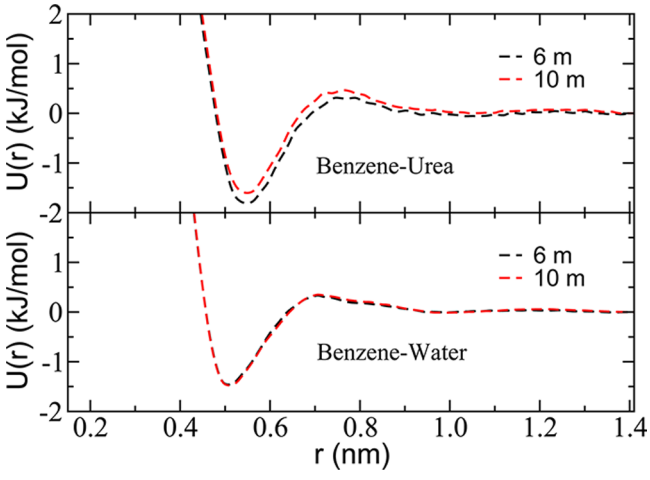

Figure 1. Single-site KB-IBI solute−solvent potentials used in CG MD simulations of 6−12 m aqueous urea solutions containing one benzene molecule.

For all the concentrations of urea, the RDFs and KBIs between benzene and urea and between benzene and water were reproduced in agreement with the atomistic model. Figure 2 shows the RDF between benzene and urea at 6 m urea concentration, both from atomistic and CG simulations, and the corresponding running KBIs as a function of distance. Similarly, Figure 3 shows the RDF and the corresponding running KBIs between benzene and water at 6 m urea concentration. The KBI between benzene and urea exceeds the KBI between benzene and water, which indicates stronger affinity between benzene and urea over that between benzene

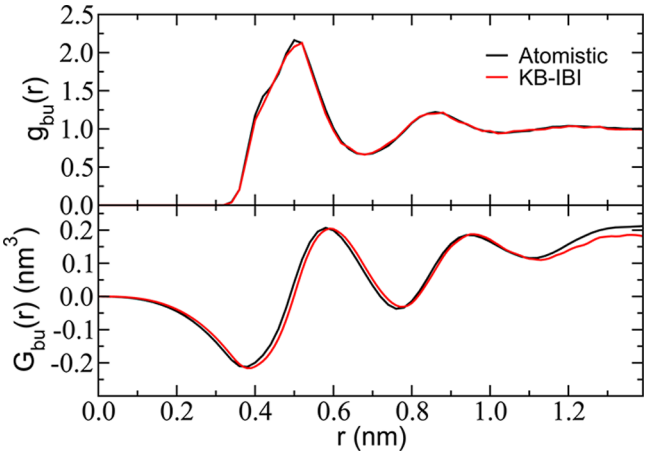

Figure 2. Radial distribution functions $g_{bu}(r)$ and running KBIs between benzene and urea for a single benzene molecule in 6 m urea−water solution. Urea−urea, urea−water, and water−water potentials were obtained by KB-IBI from an atomistic simulation trajectory of 6 m urea in water;[28] benzene−urea and benzene−water potentials were newly parametrized using KB-IBI from simulations of a single benzene molecule in 6 m urea−water solution.

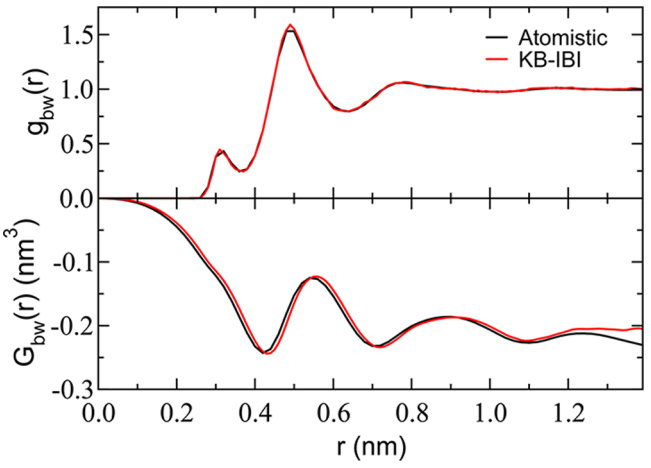

Figure 3. Radial distribution functions $g_{bw}(r)$ and running KBIs between benzene and water for a single benzene molecule in 6 m urea−water solution. Urea−urea, urea−water, and water−water potentials are obtained by KB-IBI from an atomistic simulation trajectory of 6 m urea in water;[28] benzene−urea and benzene−water potentials were newly parametrized using KB-IBI from simulations of a single benzene molecule in 6 m urea−water solution.

and water. So using eq 3 it confirms the fact that benzene is salted-in by urea in water.

The solvent/cosolvent RDFs were also well reproduced in agreement with the atomistic model though the solvent/cosolvent models were not reparameterized after the insertion of the single solute molecule. Figure 4 shows the KBIs between urea−urea, urea−water and water−water for the system of 1 benzene in 6 m urea−water solution, both atomistic and CG. Good agreement is found, as expected, because the solvent/cosolvent RDFs and KBIs do not deviate significantly from those of a pure urea−water solution at 6 m urea concentration.[28] The derivative of the solvation free-energy of benzene with respect to the urea concentration at 6 m urea was calculated using eq 3. The value of $(\partial\Delta G_b/\partial x_u)_{p,T}$ obtained from the CG simulation with benzene (−22.1 kJ/mol) agrees well with the result from atomistic simulation (−23.4 kJ/mol).

dx.doi.org/10.1021/ct400242r | J. Chem. Theory Comput. 2013, 9, 5247−5256

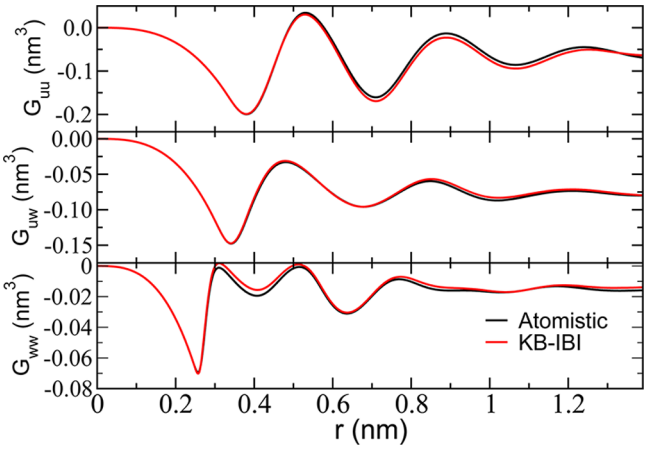

Figure 4. Running KBIs between urea−urea (uu), urea−water (uw), and water−water (ww) for a single benzene molecule in 6 *m* urea−water solution. Urea-urea, urea−water, and water−water potentials were obtained by KB-IBI method from binary mixture of 6 *m* urea in water;[28] benzene−urea and benzene−water potentials were newly parametrized from single benzene molecule in 6 *m* urea−water using KB-IBI.

For the simulations of 1 benzene molecule in 8 *m* urea−water we used urea−urea, urea−water and water−water CG potentials derived for a binary 6 *m* urea−water solution (as mentioned earlier) and parametrized benzene−urea and benzene−water potentials using KB-IBI. Figure S2 shows that the benzene−urea and benzene−water KBIs are reproduced, and the solvent−solvent KBIs are also in satisfactory agreement with the atomistic simulation results (Figure S3). The derivative of the solvation free-energy of benzene with urea concentration at 8 *m* urea (AA: −9.3 kJ/mol) is also closely reproduced (CG: −9.9 kJ/mol). Further, benzene−urea and benzene−water potentials were parametrized at 10 and 12 *m* urea concentration using a fixed solvent model derived for the binary 10 *m* urea−water solution, and the representability of the model was validated in terms of reproducing the KBIs and the variation of solvation free-energy of benzene (see Figures S4 and S5). The derivatives of the benzene solvation free-energies with urea concentration are listed in Table 1.

4.2. Salting-in of Benzene at Finite Concentrations. To study salting-in of solutes at finite solute concentrations, the additional interaction that comes into play is the solute−solute interaction. To find the solute−solute interaction, we followed two procedures: (1) taking the solvent−cosolvent interactions from the binary urea−water system while using the solute−solvent/cosolvent interactions from the systems of one solute in urea−water (described in the previous section) and using KB-IBI to find the solute−solute interaction or (2) taking the solvent−cosolvent interactions from the binary urea−water system and using KB-IBI to parametrize solute−solute, solute−solvent, and solute−cosolvent interactions. To test both procedures, we studied a system of 0.25 *m* benzene in 6 *m* urea−water (50 benzene molecules, 11111 water, and 1200 urea molecules). Figure S6 shows the KBIs between benzene−urea, benzene−benzene, and benzene−water obtained using the first method. As we only iteratively updated the benzene−benzene potential using KB-IBI, while keeping all other interactions unaltered, the KBI between benzene−benzene was reproduced in agreement with the AA result, but benzene−urea and benzene−water running KBIs could only be reproduced at distances smaller than 0.8 nm, while discrepancies were observed in the larger distance region. This is due to the fact that the atomistic KBIs between benzene−urea and benzene−water are significantly different at infinite benzene dilution and at finite concentration of benzene. The KB-IBI solute−solvent potentials thus show limited transferability. The solvent/cosolvent RDFs and KBIs were however reproduced, as shown in Figure S7, indicating that the fixed KB-IBI solvent model is transferable to finite solute concentrations. For finite concentrations of benzene we calculated the derivative of the benzene chemical potential (μ_b) with respect to the change in the number of urea molecules (N_u) using[30]

$$\mu_{bu} = \left(\frac{\partial \mu_b}{\partial N_u}\right)_{N_b,N_w,p,T} = \frac{k_B T[1 + \rho_w(G_{bu} + G_{ww} - G_{bw} - G_{uw})]}{V\eta^{finite}} \quad (4)$$

where k_B is Boltzmann constant and η^{finite} is given by

$$\eta^{finite} = \rho_b + \rho_u + \rho_w + \rho_b\rho_u\Delta_{bu} + \rho_u\rho_w\Delta_{uw} + \rho_b\rho_w\Delta_{bw} - \frac{1}{4}\rho_b\rho_u\rho_w(\Delta_{bu}^2 + \Delta_{uw}^2 + \Delta_{ww}^2 - 2\Delta_{bw}\Delta_{uw} - 2\Delta_{bu}\Delta_{bw} - 2\Delta_{bu}\Delta_{uw}) \quad (5)$$

with $\Delta_{ij} = G_{ii} + G_{jj} - 2G_{ij}$ and V being the volume of the system. μ_{bu} for the CG system was −0.00239 kJ/mol which compares with the atomistic simulation result of −0.00187 kJ/mol.

To test the transferability of the model with different urea and benzene concentrations, we have applied these CG potentials to 4 and 8 *m* urea−water solutions (with 0.25 *m* benzene) and to 6 *m* urea−water solution with 0.5 *m* benzene. For all the systems benzene−urea KBIs were significantly overestimated, and benzene−water KBIs were slightly underestimated. The solute−solute KBIs also showed deviations from AA simulations. The solvent KBIs (urea−urea, urea−water, and water−water) were reproduced reasonably except for the urea−urea KBI at 4 *m* urea concentration which shows the limitation in the transferability of the CG binary urea−water model. The corresponding KBIs and the derivatives of the chemical potential of benzene with varying solution composition are listed in Table 1 (see footnote *f*).

The second method where we updated all three potentials, namely between benzene−urea, benzene−water, and benzene−benzene, while again keeping the solvent/cosolvent model fixed, yielded a significantly better match with the atomistic KBIs, as expected. The results are shown in Figure S8 where all three KBIs between benzene−urea, benzene−benzene, and benzene−water are well matched to the atomistic ones. The urea−urea, urea−water, and water−water KBIs were also in agreement with their atomistic values (data not shown). The derivative of the chemical potential of benzene with varying urea number at 6 *m* urea concentration, μ_{bu}, was −0.00184 kJ/mol which was very close to the atomistic value −0.00187 kJ/mol.

Further we applied these potentials obtained from the simulations of 0.25 *m* benzene in 6 *m* urea−water to systems of 0.25 *m* benzene in 4, 6, and 8 *m* urea−water and also to systems of 0.5 *m* benzene in 4, 6, and 8 *m* urea−water to test the transferability of our potentials with different solute and cosolvent concentrations. The CG benzene−urea KBIs were found to be slightly off in comparison to their atomistic

dx.doi.org/10.1021/ct400242r | J. Chem. Theory Comput. 2013, 9, 5247−5256

counterparts, but benzene−water, urea−urea (except for 4 *m* urea concentrations), urea−water, and water−water KBIs were well reproduced. The benzene−benzene KBIs suffer from poorer statistics (for both atomistic and CG simulations) and were not for all the systems well reproduced by the CG potentials, although the mismatches in the benzene−benzene KBIs do not affect the results significantly while calculating the thermodynamic quantities like the derivative of the chemical potential of benzene as the concentration of benzene is very low (see eq 4). The derivatives of the chemical potential of benzene were closely reproduced for almost all the systems when compared to the atomistic values (results listed in Table 1, see footnote *g*). For 0.5 *m* benzene in 6 *m* urea−water the KBIs between benzene−urea, benzene−water, and benzene−benzene are shown in Figure 5. To verify the transferability of

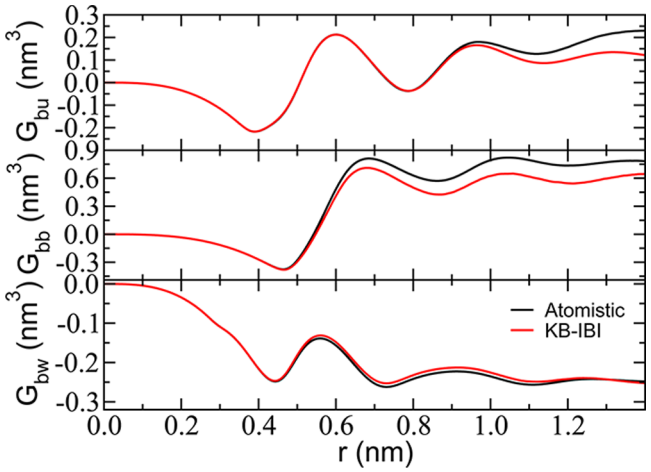

Figure 5. Running KBIs between benzene−urea (bu), benzene−benzene (bb), and benzene−water (bw) for 0.5 *m* benzene in 6 *m* urea−water solution. Here all three potentials between benzene−urea, benzene−benzene, and benzene−water are updated using KB-IBI at 0.25 *m* benzene in 6 *m* urea−water solution. Urea−urea, urea−water, and water−water potentials are obtained by KB-IBI method from binary mixture of 6 *m* urea in water.

the KB-IBI potentials obtained at a finite concentration of solute to the systems with infinite dilution of solute, we also applied this set of potentials to a system of 6 *m* urea−water containing a single molecule of benzene, and we found benzene−urea and benzene−water KBIs were in reasonable agreement with AA results. This result is particularly interesting as benzene−urea and benzene−water CG potentials which were parametrized at infinite dilution of benzene showed relatively poorer transferability when applied to a system of finite benzene concentration, but the solute−solvent potentials obtained at a finite concentration of benzene yield much better transferability to a system with infinite solute-dilution.

4.3. Cluster Analysis of Benzene in Urea−Water Solution. Benzene, at low concentration in water, forms hydrophobic clusters.[42] Addition of urea to benzene−water systems disfavors the formation of clusters as urea preferentially solvates the benzene solutes thereby reducing the hydrophobic aggregation of benzene in the solution.[43] In this section, we examine the representability of the CG model and compare clustering data with results obtained from AA simulations. The free-energy of benzene cluster growth can be defined as

$$\Delta G_{\text{growth}} = -RT \ln \frac{[n_{S+1}]C_0}{[n_S][n_1]} \tag{6}$$

where $[n_S]$ denotes the average equilibrium concentration of clusters of S benzene molecules with C_0 being the unit of the concentration. If urea disfavors clustering of benzene in water, then one can expect ΔG_{growth} to increase with increasing urea concentrations. A cluster analysis was carried out at a higher benzene concentration (0.5 m) in urea−water with different urea concentrations (4, 6, and 8 *m*). The average numbers of clusters of size S per frame were calculated using a distance criterion for the clustered benzene molecules. The cutoff distance to find the benzene molecules belonging to a cluster was chosen to be 0.73 nm, which corresponds to the first minimum after the first peak of the benzene−benzene RDFs. The solvent−cosolvent CG model was taken from pure 6 *m* urea−water solution, and the benzene−benzene, benzene−urea, and benzene−water potentials were taken from the simulations of 0.25 *m* benzene in 6 *m* urea−water by updating benzene−benzene, benzene−urea, and benzene−water potentials (mentioned as second method in the previous section and by footnote *g* in Table 1). The logarithm of the average numbers of clusters (n_S) with the cluster-size (S) is plotted in Figure 6 for three urea concentrations. We find that the

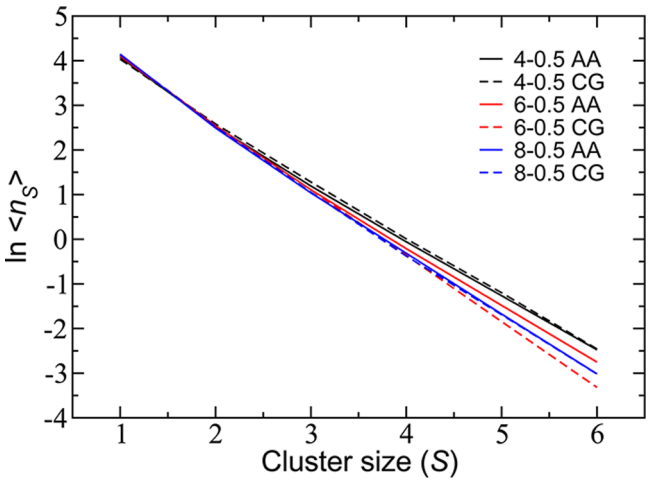

Figure 6. Logarithm of the average numbers of the benzene clusters per frame with the size of the cluster in urea−water solutions. AA and CG (KB-IBI, solute−solute, and solute−solvent potentials are obtained from 0.25 *m* benzene in 6 *m* urea−water solution; see footnote *g* in Table 1). The numbers in the legends represent the concentrations (in molality) of urea and benzene respectively.

atomistic and CG results are in reasonable agreement with each other, though the CG models were not parametrized based on these quantities. For 6 *m* urea concentration, we see that the results from the CG model slightly deviate from the atomistic ones for the cluster sizes 4 or bigger. But we see an overall decrease in the number of clusters with increasing urea concentration. Further we calculated the free-energy of cluster growth using eq 6. The results are plotted in Figure 7 for the atomistic and CG force-field models. For all the urea concentrations, good agreement between the KB-IBI and atomistic results can be observed. When compared with the results obtained from the IBI method (only solute−solute and solute−solvent potentials are obtained from 6 *m* urea−water solution with 0.25 *m* benzene using the IBI method; urea−urea,

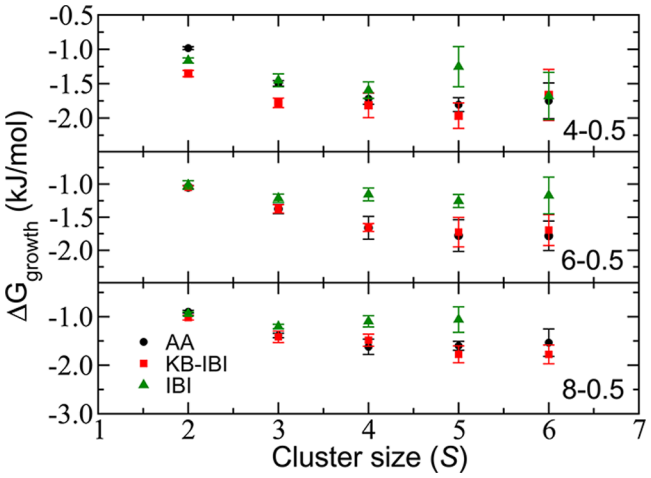

Figure 7. Free energy of benzene cluster growth versus cluster size in urea–water solutions. The numbers in the labels represent the concentrations (in molality) of urea and benzene, respectively. The CG potentials are obtained using IBI and KB-IBI, where solute–solute and solute–solvent potentials are obtained from 0.25 *m* benzene in 6 *m* urea–water solution. The KB-IBI-derived solvent model for a 6 *m* urea in water solution was used in all calculations.

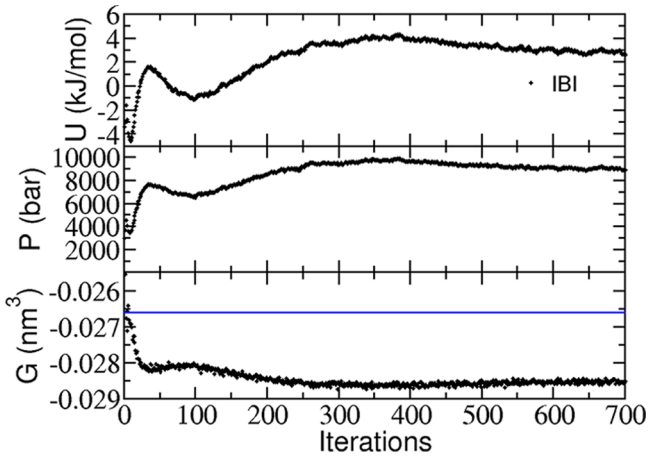

Figure 8. Thermodynamic properties of single-site CG water model obtained from IBI method. Shown are the average pair-potential per molecule (upper panel), pressure of the system (middle panel) and the KBI between the water molecules (lower panel). The single-site IBI model for pure water shows very slow convergence in the thermodynamic properties with iterations. The pressure amounts to ≈10 000 bar which is much higher than the AA simulations (1 bar). Also the water–water KBI, which is related to the isothermal compressibility, does not converge to the AA value (shown with the blue horizontal line).

urea–water, and water–water potentials are obtained from 6 *m* urea–water solution using KB-IBI) we find that IBI potentials overestimate the free-energy of the growth of the benzene clusters for the bigger cluster sizes. The free-energies of the benzene cluster growth in benzene–water systems are plotted in Figure S9 for 0.2 and 0.5 *m* benzene concentrations, where the CG potentials are obtained from KB-IBI of pure benzene–water solutions at 0.2 *m* benzene concentration. Overall we find an increase in the free-energy of the growth of the benzene clusters (at 0.5 *m* benzene concentration) with increasing urea concentrations, which also shows that urea disfavors the formation of benzene clusters and makes benzene more soluble in water. The relatively large error bars in the estimation of the free-energies can be explained by two possible causes: (1) the bigger clusters suffer from poor sampling as they occur rarely and/or (2) the sampling time for the atomistic/CG simulations was not enough.[44]

4.4. Structure-Based Coarse-Graining with Additional Thermodynamic Targets. In this section we discuss some aspects of applying thermodynamic constraints in the IBI and KB-IBI methods. Pressure and isothermal compressibility are considered as additional targets for pure water, while pressure and KBIs are considered for the mixtures with urea. Further, the potentials obtained from binary urea–water mixtures using KB-IBI and pressure correction are applied to obtain solute–solvent potentials for ternary mixtures of benzene in urea–water at infinite benzene dilution.

4.4.1. Pure water. The single-site CG IBI model for pure water, parametrized based on SPC/E water using the oxygen–oxygen RDF, shows a very high pressure and a lower isothermal compressibility than the atomistic SPC/E model.[18] The isothermal compressibility is related to the water–water KBI as

$$\kappa_T = \frac{(1 + \rho_w G_{ww})}{\rho_w k_B T} \tag{7}$$

A lower isothermal compressibility of the CG model shows that the IBI potential cannot reproduce the integral of the water–water RDF (KB integrals) accurately. Figure 8 presents the water–water KBI (lower panel) of pure IBI water along with the average potential energy per molecule (upper panel) and pressure (middle panel) versus the number of IBI iterations. It can be observed that the average potential energy per molecule and the pressure of the system are not converged even after hundreds of IBI iterations. Similar convergence problems of the average potential energy per molecule have been reported in the literature.[17] The water–water KBI obtained from the IBI model is ∼6% lower than the atomistic KBI, which is shown by the blue horizontal lines in Figures 8 and 9. While the water–water RDF converges rapidly after few IBI iterations, the pair potential still changes significantly to give rise to the difference in the pressure, energy, or the KBI which are very sensitive to the tail of the pair-potential. When KB ramp corrections[28] are applied to the potential after 60 normal IBI iterations (with no further iterations being applied to match the RDFs) we find a very fast convergence of the KBI and the pressure (Figure 9, red dots). This procedure, referred to as KB-IBI in the legend of Figure 9, reproduces the KBI accurately, while the pressure is significantly reduced and closer to the pressure of the AA system (1 bar). If instead a WJK-type pressure correction[18] is applied to the IBI potentials (Figure 9, orange squares), the pressure could be restored to the pressure of the AA system approximately, but the KBI deviates from the target value. With another approach we applied KB ramp corrections after the IBI iterations, and when the KBI was converged to the target value we simultaneously applied the WJK-type pressure correction and KB ramp corrections in every iteration step. With this approach the final results (Figure 9, green triangles) show a compromise in simultaneously reproducing the KBI and the pressure. The pressure could be reduced by 1 order of magnitude, while the KBI was reproduced within 2% of the reference value. With the KB-IBI procedure[28] or with WJK pressure corrections the average potential energy per molecule converges, unlike with IBI, after very few iterations. However, application of KB ramp corrections together with pressure corrections results in slower convergence of the potential

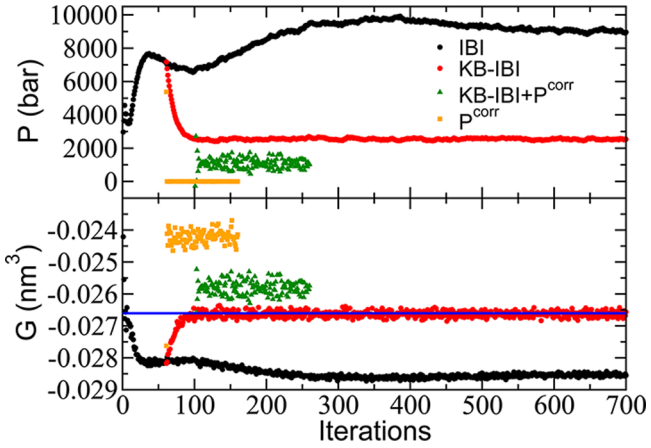

Figure 9. System pressure (upper panel) and the water−water KBI (lower panel) for single-site CG model for water. Black dots are the IBI results (same as in Figure 8). Red dots are the results obtained with the KB-IBI method, applied after 60 IBI iterations; it can be observed that KBIs converge to the AA value (shown in blue horizontal line) with the KB-IBI method. Orange squares represent the results obtained by using a pressure correction to the IBI potential after 60 normal IBI iterations; the pressure of the system rapidly converges to a value around 1 bar with pressure correction. Green triangles show the data obtained by simultaneously applying KB ramp and pressure corrections after performing 60 normal IBI steps and then 40 normal KB-IBI steps.

energy, but the running average of the potential energy with iterations does not vary much unlike IBI. The corresponding data are plotted in Figure S10.

4.4.2. Binary Urea−Water Mixture. Similar to the system of pure water, IBI or KB-IBI models for binary mixtures of urea−water also show very high pressures of the order of a few thousand bar. These unphysical high pressures may cause the system to behave as a highly compressed fluid (rather than a liquid) and may affect processes which depend on pressure and volume fluctuations. In order to parametrize single-site CG models for urea−water mixtures which reproduce the atomistic pressure, one can apply pressure-corrections to the CG potentials in a way similar to the pure water system. But from the studies with pure water we have found that simultaneously reproducing the pressure, and the KBI is not straightforward. So one may expect that for the binary mixtures of urea−water, all three KBIs, namely urea−urea, urea−water, and water−water, together with the system pressure cannot be reproduced if the combined KB-IBI and pressure correction procedure is applied to all three potentials. From eq 2 we find that the variation of the molar activity coefficient of urea with urea concentration does not depend on the water−water KBI. Also one can expect that the pressure is mostly sensitive to the water−water potential as the number of water molecules is much larger than the number of urea molecules. So in an attempt to stay consistent with the solvation thermodynamics of urea in water and to simultaneously repair the pressure, we have applied a WJK-type pressure correction to the water−water KB-IBI potential (obtained with KB-IBI of urea−water mixture) without applying any further KB-IBI corrections to it but continuing to perform KB ramp corrections to the urea−urea and urea−water potentials to reproduce urea−urea and urea−water KBIs. With these corrections (pressure-corrected KB-IBI) the system pressure reaches its target value, while urea−urea and urea−water KBIs are also reproduced. However, the water−water KBI is not reproduced as expected. The water−water KBI is in fact larger than the AA result as the addition of the attractive contributions to the potential in the pressure correction procedure leads to somewhat higher aggregation between the water molecules. The results showing the system pressure and the average potential energy per molecule versus the number of CG iterations are plotted in Figure 10 for a system of 6 *m* urea in water, and we find that the

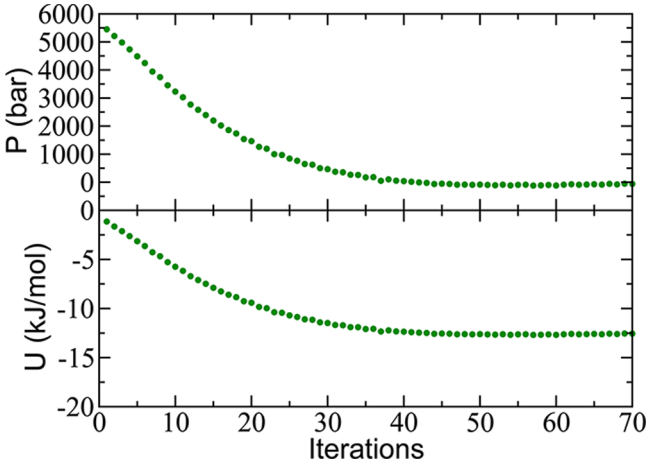

Figure 10. System pressure (upper panel) and the average potential energy per molecule (lower panel) presented against the number of iterations for a binary mixture of 6 *m* urea in water. Here we started with KB-IBI urea−urea, urea−water, and water−water potentials and applied a pressure correction to the water−water potential without any further KB-IBI correction and continued applying KB ramp corrections to the urea−urea and urea−water potentials.

system pressure and the average potential energy per molecule converge in ≈40 pressure-corrected KB-IBI iterations. In Figure 11 we plot the running KBIs between urea−urea, urea−water, and water−water obtained with the above procedure. Although the water−water KBI was not accurately reproduced, the derivative of the urea molar activity coefficient with the molar concentration of urea (eq 2) was reasonably well reproduced (−0.072 kJ/mol) with respect to the AA simulation (−0.053

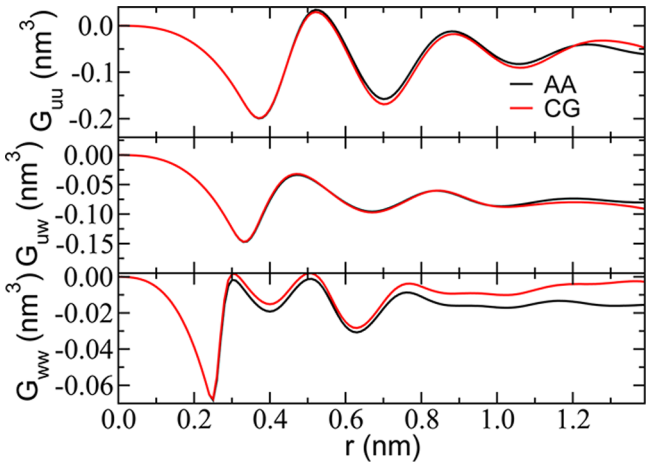

Figure 11. Urea−urea (uu), urea−water (uw), and water−water (ww) running KBIs for binary mixture of 6 *m* urea and water. Shown are the results from the AA and CG simulations with the pressure-corrected KB-IBI model parametrized at 6 *m* urea−water mixture.

dx.doi.org/10.1021/ct400242r | J. Chem. Theory Comput. 2013, 9, 5247−5256

kJ/mol). This compares to standard KB-IBI without pressure correction and standard IBI without pressure correction where −0.055 and −0.116 kJ/mol are found, respectively.[28] The newly parametrized urea−urea, urea−water, and water−water potentials are plotted in Figure S11 including a comparison with the normal KB-IBI potentials without any pressure correction.[28]

4.4.3. Benzene in Urea−Water at Infinite Dilution of Benzene. After having parametrized a pressure-corrected CG model for the binary mixture of urea and water, we applied this model to parametrize benzene−urea and benzene−water interactions to study the solvation thermodynamics of benzene in urea−water at infinite dilution of benzene. As the pressure of the binary urea−water system is close to the target pressure of 1 bar we did not apply any pressure correction to the benzene−urea and benzene−water potentials; by using standard KB-IBI the benzene−urea and benzene−water KBIs were reproduced with respect to the atomistic simulations. Figure 12 shows the

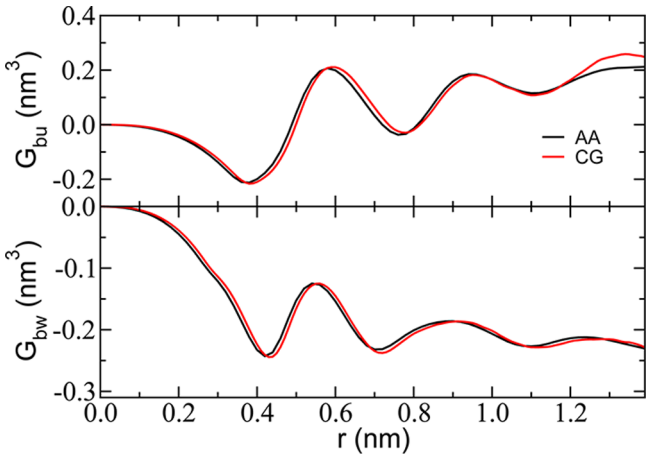

Figure 12. Running KBIs between benzene−urea (bu) and benzene−water (bw) for a single molecule of benzene in 6 *m* urea−water solution. Here the potentials between benzene−urea and benzene−water are updated using KB-IBI with single benzene molecule in 6 *m* urea−water solution. Urea−urea, urea−water, and water−water potentials are obtained by KB-IBI method from binary mixture of 6 *m* urea in water with pressure correction to the water−water potential; AA and CG.

benzene−urea and benzene−water KBIs obtained from the CG simulation and their comparison with the atomistic results. Values of all the KBIs and the derivative of the solvation free-energy of benzene with varying urea concentration are reported in Table 1 (see footnote *h*) and show reasonable agreement with the atomistic values irrespective of the fact that the water−water KBI is not well-reproduced. The benzene−urea and benzene−water effective pair potentials differ significantly from the corresponding potentials obtained with the binary KB-IBI solvent model of urea−water without pressure correction. The benzene−urea and benzene−water potentials for the two different solvent models are plotted in Figure S12.

5. CONCLUSIONS

Using the recently introduced KB-IBI method,[28] we have developed single-site CG force-fields for benzene in urea−water which reproduce the preferential urea solvation and salting-in of benzene in agreement with the parent atomistic model. Using a fixed set of urea−water CG solvent potentials previously derived based on simulations of binary urea−water mixtures, solute−solvent and solute−cosolvent potentials have been newly parametrized. Solute−solute potentials for benzene at finite concentrations in urea−water solutions have further been derived in combination with the same CG solvent model and were used in CG MD simulations at different benzene concentrations to test the transferability of the derived models. The urea/water binary solvent model was found to be transferable to systems with finite solute concentrations as evidenced by the agreement of the solution structures and the derivatives of the benzene chemical potentials with the number of urea molecules in CG and atomistic simulations. A cluster analysis of benzene in urea−water solutions at finite concentrations of benzene was furthermore performed based on which the free-energy of cluster growth was calculated at different urea concentrations with the detailed-atomistic and KB-IBI models. The simulations indicate that urea disfavors clustering of benzene, both, with the atomistic and KB-IBI models. The free energies of benzene clustering as predicted with the CG model were in qualitative agreement with the predictions of the detailed-atomistic model.

Inverse methods for molecular coarse graining include inverse Monte Carlo,[47] Newton inversion,[9] IBI,[14,15] and KB-IBI.[28] All of these methods parametrize an effective pair potential by means of iterations that aim at achieving agreement between structural target functions (usually the radial distribution functions) in the atomistic and CG systems. Because these target quantities are mostly determined by the short-range repulsive part of the effective pair potentials, with a weaker dependence on the longer-range tails, additional target quantities such as pressure and energy can be included in the parametrization. These properties are sensitive to the tails of the potentials and can, at least in principle, readily be included in the iterative procedure. Since, however, pressure and energy are not uniquely determined by the pair potential, application of these thermodynamic targets in IBI or KB-IBI may however cause that properties such the isothermal compressibility or KBI are reproduced less accurately. It is shown in this work that combined application of KBI corrections and pressure corrections during the iterative optimization leads to a good compromise in reproducing the RDF, compressibility, and the pressure for pure water with single-site CG models. For solution mixtures, the same can be achieved for the RDFs, KBIs, and pressure. Using urea−water mixtures as model systems, it was shown that by applying pressure corrections to only the water−water pair potential during the iterative optimization of the single-site models leads to rapid convergence of the RDFs, KBIs, and pressure. Moreover, since no corrections are made to any of the effective pair potentials involving the urea molecules, urea−urea, urea−water, and urea−solute KBIs can be reproduced, thus keeping a consistent description of the solvation thermodynamics in systems with dissolved solutes. With this approach, it could be shown that the salting-in behavior of benzene in urea−water can be described with single-site CG models of the solute and solvent components in good agreement with the detailed atomistic model. This shows that the KB-IBI approach to molecular coarse-graining provides models with improved properties that represent a compromise between structural and thermodynamic consistency.

Structure-based CG models are often found to be strongly state-point dependent due to inclusion of averaged multibody contributions in the effective pair potentials. In comparison to

free-energy based systematic coarse-graining methods[2] or top-down CG models such as the MARTINI model,[45] IBI-based models represent the liquid structure better by construction. The KB-IBI method improves the state-point representability in comparison to standard IBI models as it reproduces the KBIs correctly, too. Other structure-based methods such as Newton inversion[9] have been reported to reproduce the KBIs of ionic liquids.[46] Although Newton inversion or inverse Monte Carlo methods[47] applied to complex fluids show better convergence than IBI and may therefore show better agreement of the KBIs, they involve additional computational cost and require longer simulation trajectories in order to achieve reasonable statistics needed to calculate the cross-correlations.[41] The results in this paper show that the KB-IBI method converges very rapidly when applied to solution mixtures, while it provides CG binary solvent models that can readily be combined with KB-IBI models for solute−solvent and solute−solute interactions for specific solutes. The method may therefore potentially be used in future CG simulations of more complex multicomponent systems.

■ ASSOCIATED CONTENT

Supporting Information

The Supporting Information file includes additional plots showing all the newly parametrized CG potentials for the binary urea−water mixtures and ternary benzene−urea−water mixtures, running KBIs for the systems of single benzene molecule in 8, 10 and 12 m urea−water mixtures (atomistic and KB-IBI), running KBIs for the system of 0.25 m benzene in 6 m urea−water mixture (atomistic and KB-IBI), free-energy of cluster-growth of benzene for benzene-water binary mixtures and benzene-urea-water ternary mixtures (atomistic and KB-IBI), and the convergence of the average potential energy per molecule with CG iterations for a system of pure-water (IBI, KB-IBI and pressure correction). This material is available free of charge via the Internet at http://pubs.acs.org.

■ AUTHOR INFORMATION

Corresponding Author

*E-mail: vandervegt@csi.tu-darmstadt.de

Notes

The authors declare no competing financial interest.

■ REFERENCES

(1) Riniker, S.; Allison, J. R.; van Gunsteren, W. F. *Phys. Chem. Chem. Phys.* **2012**, *14*, 12423.
(2) Brini, E.; Algaer, E.; Ganguly, P.; Li, C.; Rodriguez-Ropero, F.; van der Vegt, N. F. A. *Soft Matter* **2013**, *9*, 2108.
(3) Saunders, M. G.; Voth, G. A. *Annu. Rev. Biophys.* **2013**, *42*, 73.
(4) Ingólfsson, H. I.; Lopez, C. A.; Uusitalo, J. J.; de Jong, D. H.; Gopal, S. M.; Periole, X.; Marrink, S. J. *Wiley Interdiscip. Rev.: Comput. Mol. Sci.* **2013**, DOI: 10.1002/wcms.1169.
(5) Izvekov, S.; Voth, G. A. *J. Chem. Phys.* **2005**, *123*, 134105.
(6) Wang, Y.; Izvekov, S.; Yan, T.; Voth, G. A. *J. Phys. Chem. B* **2006**, *110*, 3564.
(7) Fritz, D.; Harmandaris, V. A.; Kremer, K.; van der Vegt, N. F. A. *Macromolecules* **2009**, *42*, 7579.
(8) Villa, A.; van der Vegt, N. F. A.; Peter, C. *Phys. Chem. Chem. Phys.* **2009**, *11*, 2068.
(9) Lyubartsev, A.; Mirzoev, A.; Chen, L. J.; Laaksonen, A. *Faraday Discuss.* **2010**, *144*, 43.
(10) Hills, R. D., Jr.; Lu, L.; Voth, G. A. *PLoS Comput. Biol.* **2010**, *6*, e1000827.
(11) Carmichael, S. P.; Shell, M. S. *J. Phys. Chem. B* **2012**, *116*, 8383.
(12) Mukherjee, B.; Delle Site, L.; Kremer, K.; Peter, C. *J. Phys. Chem. B* **2012**, *116*, 8474.
(13) Brini, E.; van der Vegt, N. F. A. *J. Chem. Phys.* **2012**, *137*, 154113.
(14) Soper, A. K. *Chem. Phys.* **1996**, *202*, 295.
(15) Reith, D.; Pütz, M.; Müller-Plathe, F. *J. Comput. Chem.* **2003**, *24*, 1624.
(16) Henderson, R. L. *Phys. Lett.* **1974**, *A49*, 197.
(17) Potestio, R. *JUnQ* **2013**, *3*, 13.
(18) Wang, H.; Junghans, C.; Kremer, K. *Eur. Phys. J. E* **2009**, *28*, 221.
(19) Fu, C.-C.; Kulkarni, P. M.; Shell, M. S.; Leal, L. G. *J. Chem. Phys.* **2012**, *137*, 164106.
(20) Dill, K. A.; Shortle, D. *Annu. Rev. Biochem.* **1991**, *60*, 795.
(21) Schwarzinger, S.; Wright, P. E.; Dyson, H. J. *Biochemistry* **2002**, *41*, 12681.
(22) Bennion, B. J.; Daggett, V. *Proc. Natl. Acad. Sci. U.S.A.* **2003**, *100*, 5142.
(23) Stumpe, M. C.; Grubmüller, H. *J. Am. Chem. Soc.* **2007**, *129*, 16126.
(24) Trzesniak, D.; van der Vegt, N. F. A.; van Gunsteren, W. F. *Phys. Chem. Chem. Phys.* **2004**, *6*, 697.
(25) Lee, M. E.; van der Vegt, N. F. A. *J. Am. Chem. Soc.* **2006**, *128*, 4948.
(26) Auton, M.; Holthauzen, L. M. F.; Bolen, D. W. *Proc. Natl. Acad. Sci. U.S.A.* **2007**, *104*, 15317.
(27) Canchi, D. R.; Paschek, D.; Garcia, A. E. *J. Am. Chem. Soc.* **2010**, *132*, 2338.
(28) Ganguly, P.; Mukherji, D.; Junghans, C.; van der Vegt, N. F. A. *J. Chem. Theory Comput.* **2012**, *8*, 1802.
(29) Kirkwood, J. G.; Buff, F. P. *J. Chem. Phys.* **1951**, *19*, 774.
(30) Ben-Naim, A. *Molecular Theory of Solutions*; Oxford University Press: New York, 2006.
(31) Hovorka, Š.; Dohnal, V.; Carrillo-Nava, E.; Costas, M. *J. Chem. Thermodyn.* **2000**, *32*, 1683.
(32) Lindahl, E.; Hess, B.; van der Spoel, D. *J. Mol. Model.* **2001**, *7*, 306.
(33) Weerasinghe, S.; Smith, P. E. *J. Phys. Chem. B* **2003**, *107*, 3891.
(34) van Gunsteren, W. F.; Billeter, S. R.; Eising, A. A.; Hünenberger, P. H.; Krüger, P.; Mark, A. E.; Scott, W. R. P.; Tironi, I. G.; *Biomolecular Simulation: The GROMOS96 Manual and User Guide*; Vdf Hochschulverlag AG an der ETH Zürich: Zürich, Switzerland, 1996.
(35) Jorgensen, W. L.; Tirado-Rives, J. *J. Am. Chem. Soc.* **1988**, *110*, 1657.
(36) Berendsen, H. J. C.; Grigera, J. R.; Straatsma, T. P. *J. Phys. Chem.* **1987**, *91*, 6269.
(37) Nose, S. *Mol. Phys.* **1984**, *52*, 255.
(38) Hoover, W. G. *Phys. Rev. A* **1985**, *31*, 1695.
(39) Parrinello, M.; Rahman, A. *J. Appl. Phys.* **1981**, *52*, 7182.
(40) Essmann, U.; Perera, L.; Berkowitz, M. L.; Darden, T.; Lee, H.; Pedersen, L. G. *J. Chem. Phys.* **1995**, *103*, 8577.
(41) Rühle, V.; Junghans, C.; Lukyanov, A.; Kremer, K.; Andrienko, D. *J. Chem. Theory Comput.* **2009**, *5*, 3211.
(42) Villa, A.; Peter, C.; van der Vegt, N. F. A. *J. Chem. Theory Comput.* **2010**, *6*, 2434.
(43) Ueda, M.; Katayama, A.; Kuroki, N.; Urahata, T. *Prog. Colloid Polym. Sci.* **1978**, *63*, 116.
(44) Ganguly, P.; van der Vegt, N. F. A. *J. Chem. Theory Comput.* **2013**, *9*, 1347.
(45) Marrink, S. J.; Risselada, H. J.; Yefimov, S.; Tieleman, D. P.; de Vries, A. H. *J. Phys. Chem. B* **2007**, *111*, 7812.
(46) Wang, Y.-L.; Lyubartsev, A.; Lu, Z.-Y.; Laaksonen, A. *Phys. Chem. Chem. Phys.* **2013**, *15*, 7701.
(47) Lyubartsev, A.; Laaksonen, A. *Phys. Rev. E* **1995**, *52*, 3730.